Cooperation between redox couples at the surface of molybdates based catalysts used for the selective oxidation of propene

M. Tonelli, L. Massin, L. Cardenas, F. Ivars-Barcelo, V. Baca, J. Millet

Cooperation between redox couples at the surface of molybdates based catalysts used for the selective oxidation of propene.

M. Tonelli[1], L. Massin[1], L. Cardenas[1], F. Ivars-Barcelo[2], V. Belliere Baca[3], J.M.M. Millet[1*]

[1] Univ Lyon, Université Claude Bernard Lyon 1, CNRS, IRCELYON - UMR 5256, 2 Av. Albert Einstein, 69626 Villeurbanne (France)

[3] Adisseo, Antony Parc 2, 10 Place Général de Gaulle, 92160 Antony, France

* Corresponding author: jean-marc.millet@ircelyon.univ-lyon1.fr

Abstract

FeMoTeO mixed oxides have been synthesized and tested as catalysts for the oxidation of propene into acrolein. In order to determine the role of their constituent metallic elements, these catalysts were characterized using bulk techniques such as TEM, XANES and Mössbauer spectroscopy, as well as surface techniques including XPS and LEIS. Our results confirmed that the active phase of these catalysts corresponds to an amorphous layer of molybdenum oxide containing Te and Fe, supported on the $Fe_2(MoO_4)_3$ phase. They also show that the addition of tellurium significantly changes the redox dynamics of the catalytic surface, since it provides a fast re-oxidation route for molybdenum species. The study of MoTeO catalysts has shown that the presence of Te centers alone is not sufficient to fully re-oxidize the molybdenum. Although tellurium plays a role in the redox reaction mechanism, XPS on fresh and used FeMoTeO catalysts did not reveal any change in its oxidation state. However, the study of MoTeO samples in the early stage of their reduction by propene revealed the simultaneous formation of Te^{2+} and Te(0) species, indicating that the Te^{4+}/Te^{2+} redox couple is involved in the redox cycle. Since Te(II) is unstable, it undergoes disproportionation, if not quickly re-oxidized, leading to metallic tellurium that is easily lost from the surface. The presence of iron provides an accessible route for the re-oxidation of tellurium, thereby restoring the Te(IV) oxidation. Since iron is unable to re-oxidize Mo(V) in the absence of tellurium, and although the usual role of tellurium is that of an α-hydrogen abstracting element, it acts as a redox bridge between iron and molybdenum. This behavior would account for the high efficiency of the FeTeMoO catalysts and shows that the three redox couples Fe^{3+}/Fe^{2+}, Te^{4+}/Te^{2+} and Mo^{6+}/ Mo^{5+} cooperate in the re-oxidation step of the Mars and van Krevelen mechanism.

Keywords: Heterogeneous catalysis, Selective Oxidation of Propene, Acrolein, Iron Molybdate, Tellurium.

Introduction

Most selective oxidation reactions catalyzed by metal oxides follow a sequence of reactions, of the type known a Mars van Krevelen mechanism. This is a two-steps mechanism (cycle) in which the adsorbed organic molecule is first oxidized in a transfer reaction involving a minimum of two electrons and the reduced oxide then is re-oxidized in a second step. Most of the catalysts used for these reactions are metallic oxides with V and/or Mo as the key redox element. However, other elements susceptible to undergo oxidation-reduction reaction include Fe, Cr, Cu (transition metals) and Bi, Sb and Te (lone-pair elements), which may play multiple roles. Both reaction steps involve the exchange of electrons between the catalyst and the substrate, necessitating the intermediate storage of electrons the latter. This suggests that the active sites for oxidation reactions with a Mars and van Krevelen-type mechanism are not isolated ions, but rather correspond to an ensemble of ions, thus leading to the molecular or supra-molecular concept of active sites which has been developed in several recent studies [1-4]. The active sites could not be defined as isolated but should correspond to an arrangement of surface atoms and reactant able to simultaneous play the role of activator of di-oxygen, of provider of selectively oxidizing oxygen atoms and of activator for C–H reactant bonds [4]. Such different and complex functions require properties than most of the time cannot be provided by only one cation type and exchange of electrons, protons or oxygen anions must intervene between these sites in a dynamic and reversible manner.

Bismuth is one of the elements found to be systematically present in these ensembles when active oxidation sites are described. It does not necessarily change its valence during catalysis but modifies the electrophilic behavior of neighboring oxygen on Mo or V that, thanks to their stereo-chemically active lone pair and increased activity for C-H bonds activation of the latter [5]. In this respect, recent studies have shown how the lone electron pair of Bi^{3+} acts on the surface of the $Bi_2Mo_3O_{12}$ catalyst during the oxidation of propene into acrolein [6]. The latter study has shown that throughout the catalytic oxidation reaction, bismuth was neither

oxidized nor reduced and remained in the form of Bi^{3+}. Bi^{3+} would intervene by electronically disturbing the environment of the neighboring molybdenum oxo group on the surface of the catalyst and thus increasing their efficiency to abstract the first hydrogen of the propene molecule. Indeed, it is the free lone pair electron of Bi^{3+} that would repel the oxygen 2p lone pair on molybdenum and destabilize the bond. In parallel a back-donation from the • Mo-O • π * orbital to the Bi 6p orbital would occur stabilizing the triplet state and lowering the singlet → triplet excitation energy and consequently lowering the transition-state barrier for hydrogen abstraction [6].

The role played by tellurium or antimony is less well defined, although it is generally accepted that the addition of tellurium to molybdenum and vanadium oxide-based catalysts results in the formation of selective partial oxidation catalysts [7-10]. When in the 4+ oxidation state and because of its lone pair electrons, tellurium acts as an α-hydrogen abstracting element probably by the same mechanism as Bi^{3+}, whereas when it is present in the form of Te^{6+}cations, it can play the role of a selective oxygen or nitrogen inserter [7,8]. Knowing that TeO_3 is a selective catalyst by itself, used for the oxidation of propene to acrolein and that Te^{6+}/Te^{4+} is a relatively accessible redox couple, several authors have assumed that in the active site tellurium should be present in the Te^{6+} oxidation state [7,11-13]. On this point, Margolis et al. used Mössbauer spectroscopy to show that in CoMoTeFeO catalysts, tellurium was present in the form of both Te^{6+} and Te^{4+}, and that Te^{6+} could still be clearly detected in the used catalysts [14]. A model of the active site was thus proposed in which Te^{6+} species was responsible for the oxygen insertion, in a manner similar to Mo^{6+} in bismuth molybdate catalysts, and Te^{4+} for α-hydrogen abstraction. In this context, it has been reported that the addition to the catalyst of a re-oxidation couple such as Fe^{3+}/Fe^{2+} in the immediate proximity of the Te^{6+} stabilized this species and decreased the loss of tellurium [6]. However, it is important to note that the presence of Te^{6+} species in several other catalysts is relatively unlikely under operational conditions, since TeO_3 spontaneously decomposes to TeO_2 above 300°C [15-17]. Furthermore,

it has been shown that TeO_2 supported on silica was also able to provide acrolein with 40% selectivity, at 60% propene conversion, indicating that Te^{4+} species can also act as an oxygen inserting element [18]. In the case of antimony similar roles are currently assigned to Sb^{5+} and Sb^{3+} with an additional role played by the α-Sb_2O_4 phase, which is easily formed at the surface of the catalysts and can initiate a synergetic effect by means of oxygen spillover [19].

In MoVTe(Sb)NbO catalysts used for propane oxidation or ammoxidation, it has been shown that Te^{4+}/Te^{2+} and Sb^{5+}/Sb^{3+} couples could be involved in the oxido-reduction of the catalysts [20-23]. Although the necessary and major role of the Te^{4+} and Sb^{3+} cations remains that of facilitating the α-hydrogen abstraction from the intermediately formed propene molecule, in order to obtain a high selectivity to acrylic acid, they may also play an important role in the re-oxidation of the active sites although in this case, re-oxidation is not rate limiting. More recently, it has been proposed that the reduction of Te^{4+} to Te^{2+} and Te(0) could generate redox active O^- radical sites, which are efficient for the activation of alkanes [24].

A recent study of the FeMoTeO multicomponent catalytic system used for the selective oxidation of propene into acrolein proposed that the active phase corresponded to an amorphous molybdenum oxide doped with tellurium and iron, supported on the $Fe_2(MoO_4)_3$ phase [25]. It is likely that very active and selective sites include all the constituent elements in close vicinity inside the layer.

In order to fully determine the specific roles of iron and tellurium, a study of the redox processes taking place during the oxido-reduction of FeTeMoO catalysts but also FeMoO and MoTeO catalysts has been undertaken and is presented in this paper. The redox state dynamics at the surface of the catalysts were studied by characterizing the catalysts before and after catalytic testing and by combining spectroscopic techniques under realistic reaction conditions, which can provide information on the oxidation state of the elements. With that respect, X-ray photoelectron spectroscopy (XPS) was a well-suited technique since it can easily identify a

change in the oxidation state of the elements, and it is possible to make quantitative evaluations of the relative abundance of each species. As a complement and in an attempt to provide a consistent interpretation of all the results, several other types of characterization were further undertaken. Low Energy Ion Scattering (LEIS) was used to determine the chemical composition of the outermost surface, and to ensure that all the elements were present to intervene in the catalytic redox cycle in the case of the FeMoTeO catalyst. XANES and Mössbauer spectroscopy (in the specific case of iron, were also used to similarly determine the possible role of the bulk material in the redox process. Finally, the response of the catalyst's surfaces to reduction under propene was studied by XPS in the absence of oxygen, in order to reveal the redox state dynamics occurring at the surface.

Experimental

Preparation of the catalysts

The iron and tellurium molybdate catalysts (FeMoO and FeMoTeO) were prepared as described elsewhere [25]. 2.15 mmol of ammonium heptamolybdate (Alfa Aesar A13766) were dissolved in 100 ml of distilled water and 10 mmol of iron nitrate nona-hydrated (Sigma-Aldrich 216828) and varying amounts of telluric acid (Aldrich 86375) were dissolved in 50 ml of water. The second solution was added at room temperature to the first one maintained under vigorous stirring (600 rpm). After 1 hour under stirring, the suspension formed from the resulting solution was evaporated under vacuum. The solid obtained was dried overnight at 120°C and calcined for 3h at 500°C. A sample has been prepared with silica employed as a dispersant agent (FeMoTe-SiO_2). In this case, 5 mmol of a commercial colloidal silica solution (Ludox AS-30) were added to the first solution. Otherwise the protocol was the same as for the preparation of FeMoO and FeMoTeO catalysts. A Catalyst with only molybdenum and

tellurium (MoTeO) has been prepared using a slightly different protocol. Stoichiometric amounts of ammonium heptamolybdate and telluric acid were dissolved in 50 mL of water to obtain a 0.6 M solution in molybdenum. The solution was kept under stirring for 30 min and finally evaporated under vacuum at 60°C. The collected samples were dried at 120°C for 12 hours and calcined in air at 500°C for 3 h. All products used for the syntheses were reagent grade and gases from the IRCELYON internal gas distribution system, were used without further purification.

Characterization techniques

The chemical composition of the catalysts was determined using an ACTIVA JOBIN YVON atomic emission spectrophotometer (ICP-AES) and their specific surface area by nitrogen physisorption at -196°C on a Micromeritrics ASAP 2020 instrument using the Brunauer- Emmett-Teller (BET) method. In certain cases, a white deposit was observed at the exit of the reactor after catalytic testing on $MoTeO_x$ and characterized by a qualitative analytical method (Tin chloride test) [26]. In detail, few milligrams of the substance were carefully scratched and transferred into a test tube. The substance was then dissolved in a 10% HCl solution and reacted with a freshly prepared 0.25M acidic solution of $SnCl_2 \cdot 2H_2O$ (98%, Sigma-Aldrich). The reaction leads either to black or blue coloration depending if the solution contains respectively tellurium or molybdenum

XRD data were measured with Bruker D8A25 X-ray diffractometer operating at 50 kV and 35 mA (Cu Kα radiation at 0.154184 nm) equipped with a Ni filter. LynxEye, 192 channels on 2.95°) fast multistrip detector was used for intensity measurements. Diffraction patterns were collected at 25°C in the 4-80° 2θ range with 0.02° 2θ step size and 2 s per increment. dwell time. TOPAS v.4.2 software package and ICSD database were used for the analysis of the X-ray patterns [27].

X-ray photoelectron spectroscopy (XPS) was performed using Al Kα monochromatized source in a commercial KRATOS AXIS Ultra DLD spectrometer. XPS high resolution spectra revealed well-resolved chemical states corresponding to Fe 2p, Fe 3p, Mo 3d, Te 3d, O 1s and C 1s levels. Each core level was decomposed into a combination of Voight functions with an overall FWHM of around 1.6 eV. In order to quantify iron species, we used Fe 3p instead of the strongest photoemission line Fe 2p. This choice is due to core-hole relaxation effects in Fe 2p the so-called satellites lines, which makes it difficult to accurately determine the iron concentration by Fe 2p core level. On the contrary to Fe3p orbital of which remaining relaxation effects were not observed. For the study, samples have been characterized before and after catalytic testing. FeTeMoO-SiO_2 and TeMoO catalysts have been studied after *in situ* reduction. For that purpose, samples were heated to the same catalytic reaction temperature of 360°C under a 50 $mL.min^{-1}$ flow of argon, and then exposed to a pulse of propene in order to obtain a controlled, and minute reduction of the surface. The reduction was performed by diluting propene in argon (using a 1:1 mixture) in the auxiliary chamber, on a sample that had been stabilized during 120 hours of operation. Before being transferred to the ultra-high vacuum chamber for XPS analysis, the sample was cooled to room temperature in an argon atmosphere, in order to minimize the likelihood of Te volatilization stimulated by the high ambient temperature and low pressure inside the chamber.

XPS analysis is sensitive up to 10 nm with an average of detection around 5 or 6 nm, which makes the XPS little sensitive to the phenomena of segregation in the extreme surface. Consequently, LEIS has been used for the purpose of determining the presence of Te in the first atomic layer. It was performed using a KRATOS ionization beam source of $4He^+$ ions with a kinetic energy between 1 and 3 keV. The experiments were carried out at the scattering angle θ 40 ≈142°. The primary beam intensity was about 200 nA, focused on an impact spot of about 0.2 mm diameter.

Transmission electron microscopy (TEM) was used to acquire images of the catalysts. The apparatus was a FEI TITAN ETEM G2 microscope, operating at 300 KV and equipped with an objective Cs aberration corrector and an energy-dispersive X-ray (EDX) analyzer (SDD X-Max 80mm^2 from Oxford Instruments TM) for elemental chemical analysis. X-ray absorption near edge structure (XANES) spectra was performed at the beamline for *in situ* X-ray spectroscopy of synchrotron facilities of the Paul Scherrer Institute in Zurich (Switzerland). The experimental conditions were set to acquire spectra of Fe, Mo at K-edges and Te at L_1-edges. In a typical acquisition, the samples were diluted with amidon (50% w/w), pelletized and analyzed in transmission mode for Fe and Mo and in fluorescence mode for Te. For in situ experiments, 10-20 mg of the catalyst were charged in a glass capillary under a C_3H_6: O_2: N_2 = 1:1.5:8.6 gas mixture (total flow: 10 ml min^{-1}). The temperature was fixed to 360°C by means of a heat gun installed above the sample. In this case, acquisitions for all the edges. were performed in fluorescence mode. Mössbauer spectra were recorded at room temperature with an in-house apparatus equipped with a 2 GBq ^{57}Co/Rh γ-ray source [28]. Hyperfine parameters (isomer shifts given with respect to αFe and quadrupolar splitting were calculated with a precision of 0.02 mm s^{-1}.

Testing of the catalysts

The oxidation of propene to acrolein was performed at atmospheric pressure between 300 and 460°C in a fixed-bed type reactor (internal diameter: 12 mm) with on-line chromatographic analysis of the reaction mixture components. [25]. The reactor was in quartz and contained 0.2-2.0 g of powdered catalyst (sieved below μm180) supported on a sintered glass. A little protection tube on the surface of the glass reactor allowed placement of a thermocouple in the catalyst bed to measure the temperature. High purity nitrogen from IRCELYON internal gas distribution system was used as a carrier gas and for oxygen and

propene N50 and N25 Air Liquide gases were respectively used. The starting reaction mixture corresponded to $C_3H_6/O_2/N_2$= 30/20/50 and the gas hourly space velocity (GHSV) was equal to 296 h^{-1}. Calculated carbon balances were higher than 98%. The catalysts did not undergo any pretreatment and were directly heated to the reaction temperature under nitrogen before the catalytic gas mixture was introduced.

Conversion of propene (A) was calculated using equation (1) and N_2 as internal standard: $X(A) = \frac{moles\ A\ after\ reaction}{moles\ A\ before\ reaction}.100..$ The selectivity for a reaction product (B) (acrolein, CO_2, CO, acrylic acid, allyl alcohol, acetaldehyde and propanal) was defined as the ratio between the moles of (B) produced during the reaction, over the moles of the reagent (A) present before the reaction. When the final product (B) has a different number of carbon atoms than the reactant (A), the selectivity was corrected by the ratio of carbon atoms between product (B) and reactant (A) as in equation $S(B) = \frac{moles\ B\ after\ reaction}{moles\ A\ before\ reaction}\frac{carbon\ atom\ B}{carbon\ atom\ A}.100$. The reaction rate ($r_i$) was calculated keeping the conversion of propene below 10%, using the following equation : $ri = \frac{PQ}{RT}\frac{1}{ms}.(-\ln(1-x))$ (3) where: P is the partial pressure of propene, Q is the total flow ($m^3.s^{-1}$) R is the gas constant ($J.K^{-1}.mol^{-1}$), T is the reaction temperature (K) *m* is the mass of the catalyst (g) S is the surface are of the catalyst ($m^2.g^{-1}$) *x* is the conversion of propene.

Results and discussion

Three types of samples were prepared: pure iron molybdate (FeMoO), iron molybdate with Te (FeTeMoO) and molybdenum oxide with Te (MoTeO). XRD analysis revealed presence of only $Fe_2Mo_3O_{12}$ phase for FeMoO only (ICSD 04-007-2787) and only MoO_3 phase (ICSD03-065-2421) for TeMoO (Fig. 1). The XRD patterns of the FeMoTeO sample with and

without SiO_2 showed mainly the $Fe_2Mo_3O_{12}$ phase with a very small quantity of MoO_3 that disappeared after catalytic testing. The main characteristics of the synthesized samples are listed in Table 1.

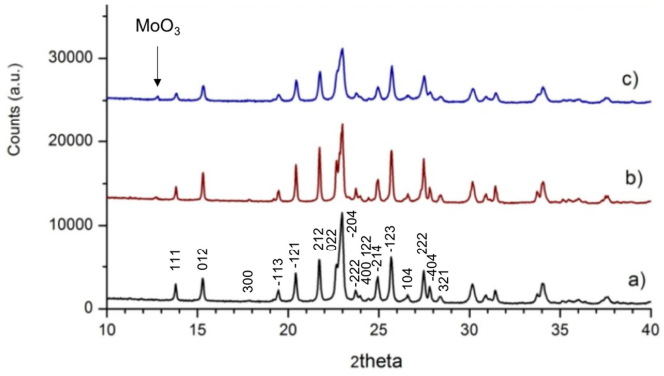

Fig. 1: X-ray diffraction patterns of the studied catalysts, a) FeMoO, b)FeMoTeO, c)FeMoTeO-SiO_2.Indexation of the peaks is given between 10 and 30°2θ.

Table 1: Results of the chemical analysis and textural characterization of the synthesized molybdates, the cationic ratios were determined by chemical analyses.

Sample [1])	Chemical composition	Te/M (M=Mo, Fe)	Fe/Mo	SSA ($m^2.g^-$
FeMoO	$Fe_2Mo_3O_{12}$	-	0.66	5.2
FeMoTeO	$Fe_2Mo_3Te_{0.1}O_x$	0.002	0.66	3.5
MoTeO	$Mo_{2.95}Te_{0.05}O_x$	0.017	-	6.7

The solids have the chosen compositions with their specific surface areas are comparable. The iron containing samples have previously been characterized by transmission electron microscopy that showed that they both exhibited a few nm thick amorphous surface layer formed during sample preparation and probably caused by incomplete precipitation of the iron species (Table 2) [25,29]. These layers which are clearly visible in Fig.2 with different image contrasts, contain all of the elements present in the samples (Table 2). In the case of the ferric

molybdate compounds, this layer was richer in molybdenum and also contained Te in the case of the FeMoTeO sample. Similar surface layers of various thicknesses have previously been reported in the case of pure $Fe_2(MoO_4)_3$ catalysts used for the partial oxidation of methanol [30-32].

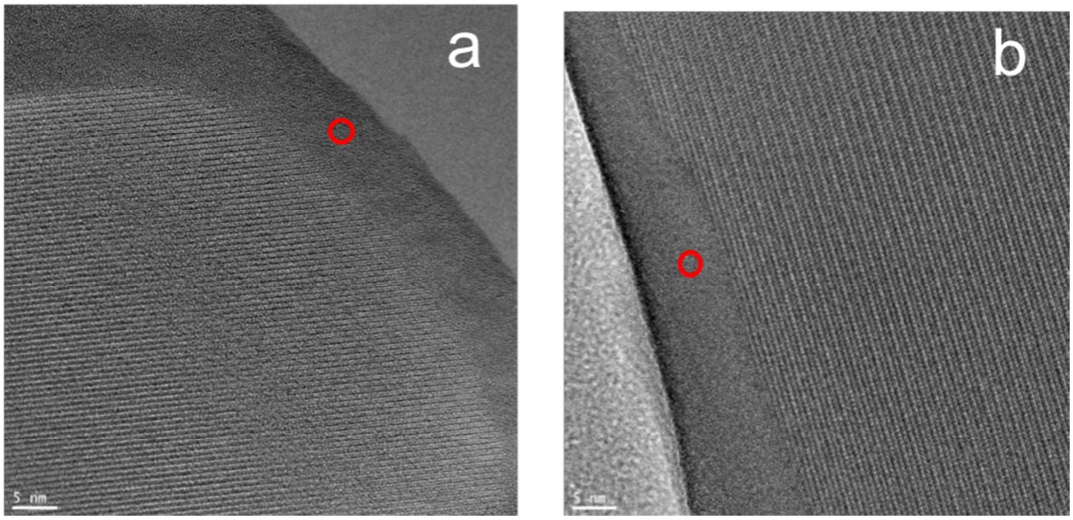

Fig. 2: TEM images of the iron containing samples a) FeMoTeO and b) FeMoO; the places where the analyses presented in Table 2 have been done are given by red circles.

Table 2: Results of EDX analyses of the amorphous layer coating the synthesized molybdates. The places were the analyses have been made are shown in Fig. 2.

Sample	Surface chemical composition	Te/(Mo+Fe)	Fe/Mo	Thickness (nm)
FeMoO	$Fe_2Mo_5O_x$	0.000	0.41	5-10
FeMoTeO	$Fe_2Mo_7Te_{0.5}O_x$	0.055	0.29	5-15

The tellurium and molybdenum mixed oxide MoTeO dit not exhibit the same surface amorphous layer but a homogeneous distribution of Mo and Te all over the crystallized oxide particles as it can be seen in Fig.3. EDX analyses gave an averaged Te/Mo cationic ratio in the phase of 0.022±0.005, which is in relatively good agreement with the one calculated from chemical analysis: 0.017 (Table 1).

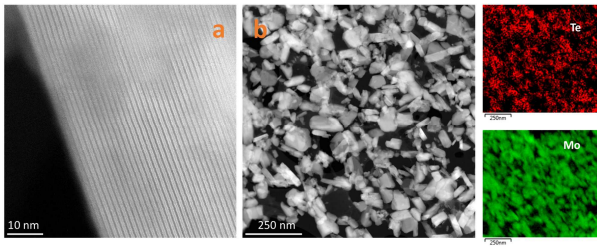

Fig. 3: a) HRTEM image of particles of the MoTeO sample. b) STEM-EDX mapping of the Te and Mo elemental distribution for an examined area.

Prior to deeper characterization, the samples were tested as catalysts under the same conditions, the results of which are listed on Table 3.

Table 3: Catalytic performances of the samples after 70h on stream. Testing conditions: $C_3H_6/O_2/N_2$= 30/20/50 with a 296 h^{-1} gas hourly space velocity (GHSV); rates of conversion of propene were calculated using the specific surface area measured after testing.

Sample	T(°C)	Conversion (%)	Selectivity (%)	Rate of conversion ($mol.s^{-1}.m^{-2}$)	($mol.s^{-1}.g^{-1}$)
FeMoO	450	34	10	3.4.	50.7
FeMoTeO	450	13	93	8.1	34.0
FeMoTeO-SiO_2	360	82	82	1.2[a]	23.8[b]
MoTeO	360	25	82	1.0	8.0

[a] this rate is only indicative since it was calculated using the total specific surface area of the solid including that of the SiO_2 dispersant.[b] this rate was calculated considering the weight of active phase only.

The evolution of the catalytic properties as a function of time of the various catalysts is shown in Fig. 4. It is found that all the catalysts undergo a loss of activity during the first hours of testing before stabilization after about 70 hours. this loss of activity was attributed mainly to sintering and is more important for the catalysts tested at higher temperatures and for Te containing catalysts since it decreased by 30 % for FeMoO and 60 % for FeMoTeO catalyst.

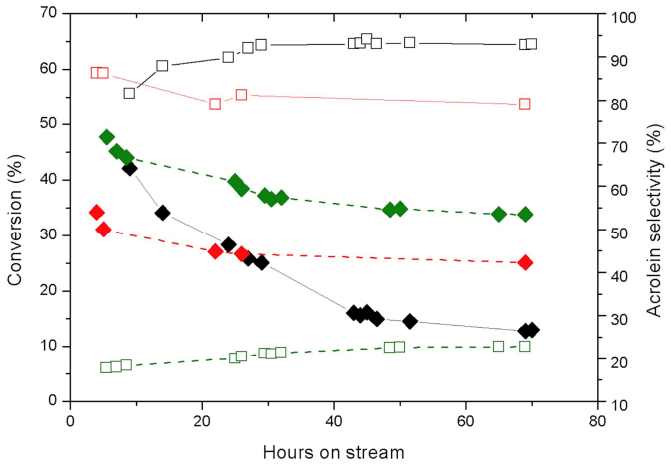

way

Fig. 4: Evolution over time on stream of the propene conversion (full diamond) and acrolein selectivity (empty squares) for the FeMoTeO sample (black) at 450°C, the FeMoO sample (green) at 450°C and MoTeO (red) at 360°C; other testing conditions: GHSV = 295 h^{-1}, $C_3H_6/O_2/N_2$ = 1:1.5:8.6.

The addition of tellurium to FeMoO has a positive effect on the activity which appears clearly when intrinsic rates of propene conversion in $mol.s^{-1}.m^{-2}$, are compared (Table 3) but also, and in a remarkable, in selectivity to acrolein which reached 93% after 70 h. These results are in agreement with those published earlier, when it is considered that the latter were obtained after only 5 hours on stream [7,33].

It is difficult to compare the catalytic properties of the MoTeO samples with those of the other samples. At 360°C the FeMoO and FeMoTeO catalysts were almost inactive whereas at 450°C the MoTeO catalyst reached total conversion and deactivated continuously with time on stream. Nevertheless, when a FeMoTeO sample was prepared with SiO_2 as a dispersant agent, it exhibited significantly smaller particles and was at 360°C as selective but more active than the MoTeO catalyst (Table 3). This higher activity is more visible when the specific propene conversion rates of the two catalysts are compared rather than their intrinsic rates. This is because the effective masses of the two catalysts can be evaluated but not their specific surface areas since in the case of the iron tellurium molybdate it includes that of silica (Table 3).

A very detailed characterization of this catalyst was published recently [25,29]. It was shown that SiO_2 nanoparticles provided a physical barrier to the sintering of the iron molybdate phase without modifying it nor affecting the amorphous layer at its surface. It should be mentioned for the $MoTeO_x$ sample, that a very slow decrease of selectivity and activity was encountered over very long time periods contrary to the iron containing catalysts that reached a real equilibrium after 70 h. Furthermore, a deposition of a white substance at the exit of the reactor, identified as a tellurium compound by reaction with tin chlorate, was observed for the $MoTeO_x$ samples. ICP-AES analysis on the fresh and used $MoTeO_x$ samples quantified the loss of tellurium to about 10% of the initial concentration. No loss of tellurium was observed using the same technique for the iron containing catalysts.

The catalysts were analyzed before and after catalytic testing, using X-ray photoelectron spectroscopy (XPS), in order to determine the oxidation state and atomic concentration of the elements at the surface as well as variation of these quantities, after catalytic testing. The results obtained are presented on Table 4 and in Fig. 3. As far as the oxidation states of the elements are concerned, Table 4 shows that in the fresh catalysts only one species of molybdenum was present, with a binding energy of 232.4 eV (Mo3d5/2 peak) was characteristic of Mo(VI) [34]. On the used FeMoO and MoTeO catalysts, a second contribution at 231.7 eV could be distinguished, and by comparison with data published in the literature, assigned to Mo(V) [34,35]. The latter species were present in considerably greater quantities on FeMoO (17.3%) than on MoTeO (3.5%). Iron, as expected, was present mainly in the form of Fe(III), as shown by the typical value of the Fe2p3/2 peak at 711.5 eV. Nevertheless, a minor contribution at 709.8 eV, characteristic of the Fe(II) species was always present, both in the fresh and the used catalysts [35-37]. Tellurium was exclusively found in the form of Te(IV), as indicated by the position of the 3d5/2 peak at 576.6 eV [10,39]. It should be noted that since tellurium was introduced during the synthesis in the form of Te(VI) as telluric acid (H_6TeO_6), the latter result implies that the Te(VI) underwent a reduction to Te(IV) during the calcination process.

Table 4: Main physical and chemical characteristics of the surface of the fresh (f) and used (u) molybdates catalysts determined from results of XPS analyses.

Sample		Binding energies (eV)					Surface atomic ratios	
		Mo 3d5/2	Mo 3d5/2	Fe 2p3/2	Fe 2p3/2	Te 3d5/2	Fe/Mo	Te/M (Mo,Fe)
FeMoO	f	232.4	-	711.4	709.3	-	0.59	-
	u	232.4	231.7	711.5	709.4	-	0.54	-
FeMoTeO	f	232.6	-	711.6	709.3	576.6	0.63	0.08
	u	232.7	-	711.5	709.3	576.6	0.60	0.09
FeMoTeO-SiO_2	f	232.5	-	711.6	709.3	576.5	0.56	0.06
	u	232.6	-	711.7	709.4	576.6	0.53	0.06
MoTeO	f	232.7	-	-		576.5	-	0.05
	u	232.7	231.7	-		576.4	-	0.14

This finding is in agreement with previous thermal and thermogravimetric analyses on H_6TeO_6, for which it has been shown that the spontaneous decomposition of telluric acid into to TeO_2, H_2O and O_2 occurs art approximately 300°C [17]. Table 4 shows that by comparison with the bulk stoichiometry, the surface of the FeTeMoO and FeMoO catalysts was enriched in molybdenum. The differences were however not as great as those generally reported in the literature for $Fe_2(MoO_4)_3$ catalysts when the Fe2p signal was used [36,40,41]. It is also interesting to note that the surface concentration of molybdenum was generally higher in the used catalysts, thus implying that some molybdenum migrates to the surface under operating conditions. Compared to the general chemical stoichiometry, an even higher enrichment with respect to the chemical stoichiometry was observed for the surface tellurium concentration. This result confirms the tendency of this element to accumulate in the outermost layer of the FeTeMoO catalysts, as previously observed by electron microscopy and in agreement with the literature [42]. Interestingly, the total concentration of Te in the bulk remained almost unchanged after catalytic testing in the FeTeMoO catalyst whereas a loss of about 10% was observed by ICP-AES for the MoTeO catalyst. These results appear in agreement with the findings of Ueda et al. concerning the fundamental role played by iron in the prevention of Te volatilization [8,43]. The observed increase in the surface Te concentration provides an explanation for the progressively stronger selectivity to acrolein as a function of time on stream

(Fig. 4). Interestingly, although Te surface content of the MoTeO sample increased, the sample exhibited a slight loss of selectivity. It cannot be excluded that in this case the degree of surface reduction also played an important role in the rate of formation of deep oxidation products. In the paragraph further down, it is shown that the surface of MoTeO was much more reduced than that of other catalysts and that the presence of iron could have a determinant role in avoid this phenomenon

A variation in the concentration of Fe(II) species was observed after catalytic testing (Fig. 5). As previously mentioned, a shoulder was systematically detected in the freshly calcined catalysts at 709.2 eV, corresponding to the signal from the Fe^{2+} species, the strength of which increased after testing. A Similar increase was reported for $Fe_2(MoO_4)_3$ in the selective oxidation of methanol to formaldehyde [37]. These authors observed an increase in the Fe^{2+} signal under reducing conditions and proposed that the iron sites intervene in the hydrogen abstraction step of the mechanism. However, in the case of the present study there was virtually no change in the intensity of the Fe^{2+} signal from the FeMoO catalyst after exposure to the propene/oxygen mixture under operative conditions, whereas a significant increase in the intensity of the Fe^{2+} signal was observed in the Te-containing catalysts after catalytic testing. Indeed, it is not necessarily true that the lattice oxygen inserted in the propene molecule arise from iron centers. Nevertheless, since Fe_2O_3 is not selective to acrolein and that an iron excess in $Fe_2(MoO_4)_3$ catalysts always results in the increased formation of combustion products, it seems more likely that the insertion of oxygen occurs on Mo centers. However, if this is the case, the formation of Mo^{5+} species should be observed on FeMoTeO catalyst, as reported for the spent $Fe_2(MoO_4)_3$ catalysts used for the oxidation of methanol.

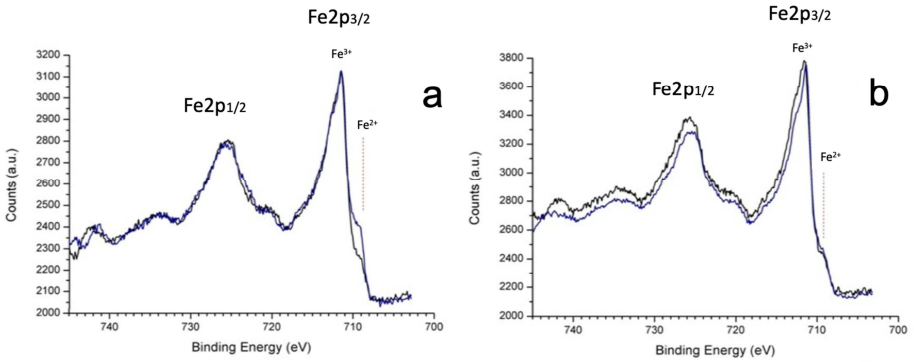

Fig. 5: XPS spectra for The FeMoTeO (a) and FeMoO (b) samples in the Fe 2p region before (in black) and after catalytic testing (in blue).

Low Energy Ion Scattering (LEIS) was used to characterize the FeMoTeO catalyst before and after catalytic testing and to determine the tellurium segregation on surface opposite to Mo/Fe ratio (Fig. 6). LEIS is currently used for quantitative determination of surface composition of the outer atomic layer. However not a trivial task is, different parameters limit the quantification and the analysis under static conditions, hence without modification of the outermost atomic layer of the surface. This type of operative mode is extremely complicated to achieve because, in addition to requiring technical conditions at the top of technology specifically, detection sensitivity and an outstanding ion source control, a prior knowledge about atomic or molecular sensitivity factor is necessary. In order to calculate this parameter, the use of ideally monocrystalline standard samples is required. Although such samples were not available at the time of this study, it was possible to compare the relative sensitivity factors of each element by using the values previously reported for Mo and Fe [44], these values are close enough to consider that the abundance obtained from their respective LEIS areas are comparable.

Fig 6b shows a LEIS spectrum carried out at 1 KeV during approx. 3 min on FeMoTeO catalyst revealing two contributions located at 790 and 850 eV one corresponding to Fe and other attributable to Mo. LEIS Mo/Fe ratio was approx. 1.1 confirmed by XPS. However, under

the conditions mentioned above it was not possible to detect the presence of tellurium, due probably to surface backscattering induced by contamination on surface. At this point an important question arises about the probability of sputtering the surface, since not all ions are backscattered a non-negligible percentage of ions will impact the surface causing damage. Ion dose was calculated in order to estimate the surface damage induce for He^+ ions (Fig. 6a), as reported before by H.H. Brongersma et al. [45], ion dose is widely used to define the threshold of destructive and static analysis, this is strongly correlated to kind of surface, low for organics ($1x10^{13}$ ion.cm^{-2}) and higher for metals ($1x10^{16}$ ion.cm^{-2}). It becomes crucial to have an idea about this physical parameter in order to find a good compromise between signal/noise and surface damage. LEIS analysis carried out between 1 and 3 KeV at different acquisition times shows ion doses calculated values ranging from approx. 10^{17} to 10^{29} ion.cm^{-2} (Fig 6a) although $6.7x10^{17}$ ion.cm^{-2} approaches the acceptable threshold in static mode it is still high to claim that no damage has been caused to the surface of the catalyst. However, at higher ion dose (10^{19} and 10^{29} ion.cm^{-2}) the damage of the surface it becomes evident by increasing Mo/Fe ratio obtained also by XPS analysis (Fig. 6a). This ratio measured by XPS and LEIS could be useful to estimate the damage caused to the surface, for instance at 3 KeV the Mo/Fe ratio increases moving away (approx. 2) from the initial composition 1.

(a)

Energy (KeV)	time (min)	ISS Mo/Fe ratio	ion current (nA)	ion dose (ion/cm2)	XPS Mo/Fe ratio	XPS Mo/Te ratio
1	3	1.1	220	6.72e+17	0.9	6.1
1	7	1.1	220	1.44e+18		
2	20	1.3	1200	2.24e+19	2.1	1.9
3	42	2.1	2500	9.83e+29	2.5	77.1

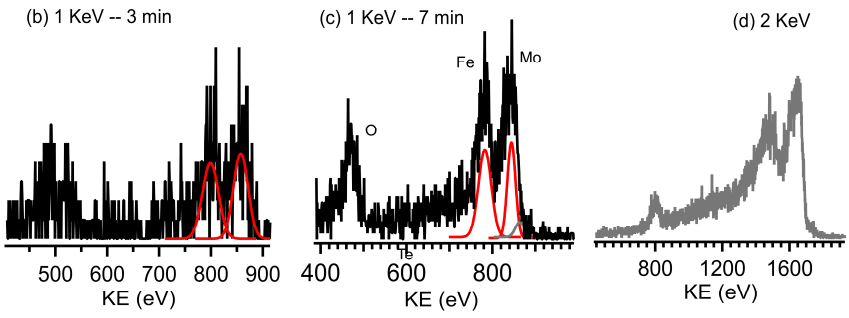

Fig. 6: Semi-quantitative surface analyses carried out by XPS and LEIS accompanied by the ion dose calculations (a). Spectra of the FeMoTeO sample collected at 1 and 2 KeV after different times (b), (c) and (d).

Subsequently, the time was increased close to 2 times (approx.7 min Fig. 6c) improving the noise/signal ratio obtaining a LEIS spectrum with a weak presence of Tellurium at 870 eV. In parallel, XPS measurements were carried out in order to gain further insight into the real elemental ratio, showing that around 10nm plus the layers removed by the ionic He^+ sputtering at 1KeV the ratio Mo/Fe remains stable around 1 (see Table 6a). From this data, it is complicated to draw a definitive conclusion about Te position. However, clearly XPS Mo/Te ratio (Table 6a) exhibit strong variations, highlighting that after a long sputtering (42 min) Te concentration is reduced drastically indicating its almost absence in deep layers of the catalyst. The opposite case was observed during the first 3 and 20 minutes of sputtering, Tellurium presence is not negligible. A detailed XPS analyses shows Te at low doses close to static mode and at higher doses in the destructive mode (see Mo/Te ratio, Table 6a), revealing thus, a tellurium distribution between the surface and intermediate layers of the catalyst.

The surface analyses (XPS and LEIS), together with the TEM results obtained on the FeMoTeO catalyst, allow a clear explanation to be given for the increase in selectivity to acrolein observed with time on stream. It was shown that the surface of the fresh catalyst presented a high concentration of Fe^{3+} species, which are responsible for the formation of deep oxidation products. This explains the very high exothermicity of the catalytic reaction in the first hours of operation, meaning that approximately 10 hours are needed before a stable target temperature is reached. As the catalyst's makeup changed, its surface was enriched in tellurium and molybdenum, this led to a decrease in the number of deep oxidation sites arising from the Fe^{3+} surface species. This is the reason for which we observed both the decrease in the number of unselective sites, and the formation of new, highly selective sites.

The catalysts were also characterized after catalytic testing, by means of X-ray Absorption Near Edge Structure (XANES) and Mössbauer spectroscopy. This provided valuable insight into the extent to which the core of the catalyst was reduced, which cannot be

determined using surface techniques. The three catalysts, FeTeMoO, FeMoO and MoTeO, were characterized at their Fe and Mo K-edges and Te L_1-edges, prior to and following catalytic testing. The XANES spectra of the fresh FeMoO sample provided reference values for the Fe and Mo K-edge of pure $Fe_2(MoO_4)_3$. The Fe K-edge is characterized by two pre-edge features at approximately 7114.3 and 7121.1 eV, labeled "A" and "B" in Fig. 7 and arising from forbidden 1s-3d dipole transitions. The edge position (C), arising from an allowed 1s-4p transition, was found at 7131.3 eV, which is in good agreement with the values reported in the literature for ferric molybdate [46]. Virtually no change was observed in the oxidation state of iron after testing (Fig. 7a). At the Mo K-edge, the spectra for the fresh and used FeMoO samples were again comparable. The pre-edge features

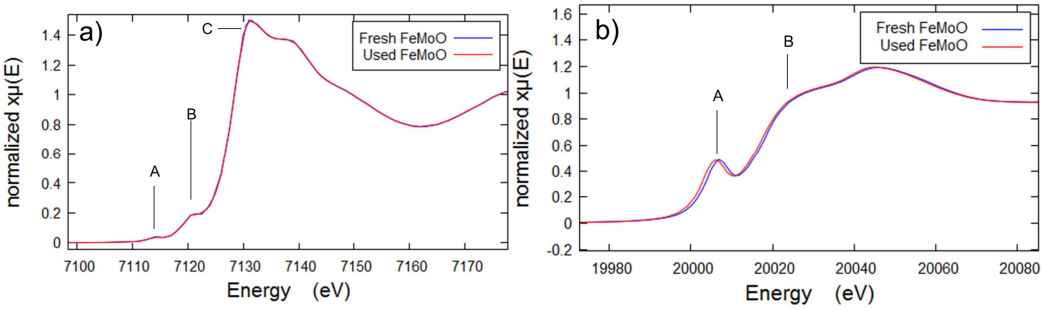

Fig. 7: XANES spectra of the fresh and used FeMoTeO sample at Fe (a) and Mo K-edge. (b)

at 20007 eV, labeled as "A" in Fig. 7b, corresponds to a 1s-4d transition, which is allowed by 4d-5p hybridization. The edge at 20029 eV (B), corresponds to an allowed 1s-5p transition, which is shifted to lower energies following reduction of the molybdenum species [47,48]. the results presented in Fig. 7b with the shift of the A and B features to lower energies, clearly show that the used FeMoO catalyst was characterized by reduced molybdenum species. These results are in agreement with the XPS analysis showing that there was no variation in the iron signal and that both Mo^{6+} and Mo^{5+} species are present in the used catalyst. They are also in agreement with the results provided by Mössbauer spectroscopy showing no reduction of iron.

The introduction of tellurium in the FeMoO catalyst lead to various changes. In Fig. 8a it can be seen that the Fe K-edge of the used catalysts decreased in intensity, whereas the intensity of the B feature increased slightly. These changes in the XANES signal can be explained by a partial and minor reduction of iron centers to Fe^{2+}. This result again confirms those obtained with XPS and Mossbauer spectroscopy. The Mo K-edge of the sample in Fig. 8b experienced a shift to lower energies, indicating that the molybdenum was reduced in the Te-containing catalyst. Although not totally surprising, this is an important result, since the XPS measurements indicated the presence of Mo^{6+} species only at the surface of the FeTeMoO catalyst.

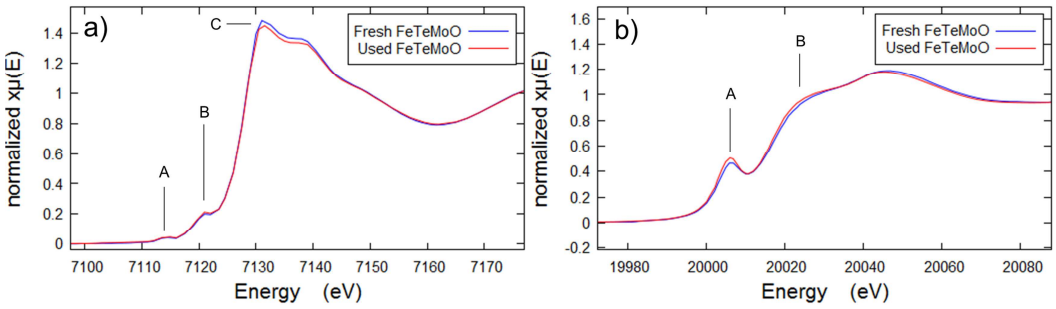

Fig. 8: XANES spectra of the fresh and used FeMoTeO sample at Fe (a) and Mo K-edge (b).

XANES spectroscopy thus demonstrated that the bulk of the FeTeMoO catalysts is involved in the redox process and that both iron and molybdenum take part in the reaction. In Fig. 8 it can also be noticed that, contrary to the case of the FeMoO sample, there is an increase in the pre-edge feature in the used catalyst. This observation can be explained but a decrease in the catalyst's octahedrally coordinated molybdenum content. Indeed, in addition to the presence of ferric molybdate, fresh FeMoTeO catalysts presented small reflections of MoO_3, which disappeared in the XRD pattern of the used samples. The disappearance of the MoO_3 phase in the XRD pattern and the simultaneous increase in the A pre-edge feature of the Mo XANES spectrum, can be explained either by the volatilization of surface MoO_3, as often observed in the oxidation of methanol to formaldehyde on $Fe_2(MoO_4)_3$ catalysts, or by the transformation of crystalline molybdenum oxide into an amorphous surface layer wetting the $Fe_2(MoO_4)_3$ phase

and in which Mo has a distorted coordination. Since chemical analysis of the used catalyst did not reveal any decrease in the molybdenum concentration whereas an amorphous layer was clearly observed using TEM analysis, the latter option appears to provide the most likely explanation. Moreover, it is possible that the transformation of the rather inactive and unselective MoO_3 into a Te and Fe-doped surface layer, contributes to the increased in selectivity to acrolein of the FeMoTeO sample. The fresh and used FeMoTeO samples were also studied at the Te L_1-edge, as shown in Fig. 9. The fresh sample exhibited two distinct peaks at 4944 and 4948 eV, corresponding to Te^{4+} and Te^{6+} species respectively [22]. We recall that XPS analysis of the fresh FeMoTeO catalyst indicated the presence of Te^{4+} species only at the surface, thus meaning that all Te^{6+} cations were confined to the bulk of the catalyst. These observations appear to confirm the EXAFS results reported by Garagiola et al., for the equivalent fresh FeTeMoO catalysts, in which Te^{6+} species were identified [49]. These authors concluded that the superior catalytic properties of the Te-doped ferric molybdate were ascribable to the stabilization of tellurium in its Te(VI) oxidation state. This conclusion was not confirmed since none of the aforementioned techniques was able to detect the presence of Te(VI) in the used catalysts. The later species is certainly present only in the fresh catalyst, and its incorporation within the ferric molybdate structure can provide a reasonable explanation for the observed segregation of molybdenum in the form of MoO_3. However, these Te^{6+} species are not stable under the operative conditions of propene oxidation and probably migrate at the surface of the catalyst where they are stabilized in the form of Te^{4+} within the outermost amorphous Mo-rich layer.

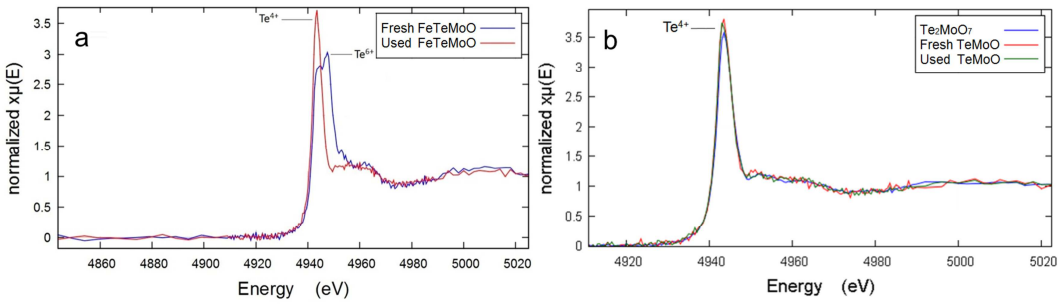

Fig. 9: XANES spectra of the fresh and used FeMoTeO (a) and of TeMoO (b) catalysts at Te L_1-edge; the spectrum of Te_2MoO_7 is added for comparison in (b).

Fig. 9 shows the XANES spectra at the Te L_1-edge of fresh and used MoTeO samples showing that tellurium was exclusively in the form of Te^{4+}. Although tellurium was introduced during the synthesis as Te^{6+}, this result implies that it was completely reduced to Te^{4+} during calcination at 400°C. Similar reduction has already been observed on the FeTeMoO catalyst. However, whereas in the latter case approximately half of the tellurium was still present as Te^{6+} in the crystalline bulk, the XANES spectra of the MoTeO catalysts indicated that the Te^{6+} signal was extremely weak, if not totally absent.

To complete the bulk characterization, the FeMoO and FeMoTeO samples were analyzed using Mössbauer spectroscopy (Fig. 10, Table 5). All of the spectra were fitted with a single ferric doublet. The hyperfine parameters computed from the fit of this doublet are consistent with high-spin Fe^{3+} in an octahedral environment and are closed to those published for pure ferric molybdate [50].

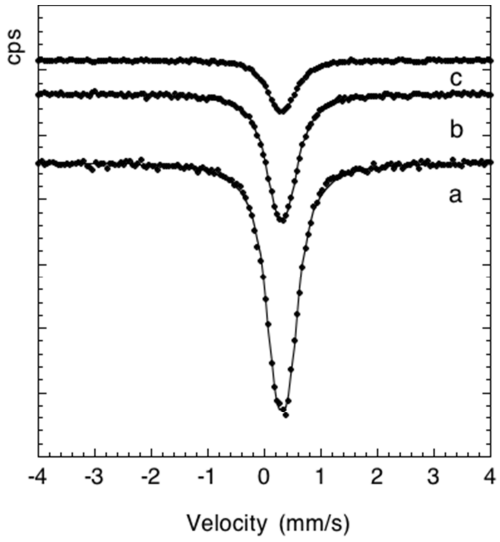

Fig. 10: Mössbauer spectra of the iron catalysts after catalytic testing a) FeMoTeO b) FeMoO c) FeMoTeO-SiO_2; solid-lines are derived from a least-squares fits.

Table 5: Hyperfine parameters calculated from the Mössbauer spectra of the iron containing catalysts recorded at 25°C. IS: isomer shift referred to αFe, W: half linewidth, QS: quadrupolar splitting.

Compound		IS (mm/s)	W (mm/s).	QS (mm/s)
FeMoO f	Fe^{3+}	0.41	0.17	0.18
FeMoO u	Fe^{3+}	0.40	0.23	0.23
FeMoTeO f	Fe^{3+}	0.40	0.18	0.19
FeMoTeO u	Fe^{3+}	0.39	0.24	0.22
FeMoTe-SiO_2 f	Fe^{3+}	0.41	0.19	0.20
FeMoTe-SiO_2 u	Fe^{3+}	0.39	0.23	0.21

After catalytic testing, the samples exhibited the same spectra. This clearly shows that the reduction evidence by XPS is limited to the surface and certainly to iron cations in the amorphous surface layer. We recall that if the reduction would have concerned the bulk, it would have induced a phase transformation that would have been detrimental to the catalytic activity:

$$Fe_2(MoO_4)_3 \longrightarrow FeMoO_4 + MoO_3 + ½\ O_2 \qquad (1)$$

The XPS study on the fresh and used catalysts described in the previous paragraphs indicates that the tellurium Te^{4+} species was present at the catalyst surface and remained in that state after testing. Molybdenum was reduced after testing in FeMoO and TeMoO catalysts, but not in FeTeMoO where it remained in its highest oxidation state. Iron, for its part, appeared to be reduced by testing on the surface of the FeTeMoO but not that of the FeMoO catalyst. It is quite likely that the insertion of oxygen into the activated propene molecule takes place essentially on Mo centers, such thus that Mo^{5+} species are formed during the catalytic reaction.

These relatively unstable species could be rapidly and specifically re-oxidized by iron cations present in close proximity in the FeTeMoO catalyst.

In order to understand the differences observed between the different catalysts, and to gain a better understanding of the redox processes involved in the oxidation of propene, XPS was used to study *in-situ* reduced FeTeMoO-SiO_2 and TeMoO samples. Figs. 11 plots the changes in the iron, molybdenum and tellurium signals, respectively, of the stabilized FeMoTeO-SiO_2 sample following exposure to a propene pulse. As long as the reduction of the surface was maintained, subsequent variations in the XPS spectra of the three metallic elements were observed: the strength of the iron peak at 709 eV increased, which is indicative of a higher concentration of Fe^{2+} species. Virtually no molybdenum signal at lower energy was detected indication that Mo^{5+} species must be present at very low concentration. Finally, the most significant effect recorded during the reduction by propene occurred with the Te signal: although the only signal observed was that of the $Te3d_{5/2}$ doublet at 576.6 eV, which is characteristic of Te^{4+}, its intensity decreased significantly. When a second pulse of propene was released, identical, but amplified changes were observed in the Fe and Mo signals, whereas the Te signal disappeared almost completely.

The *in-situ* reduction by propene of a FeTeMoO-SiO_2 catalyst showed that almost no molybdenum was reduced to Mo^{5+}, whereas the most significant changes were observed for iron and tellurium, the former being reduced into Fe(II) and the latter partially disappearing from the surface, most probably as a consequence of volatilization following its reduction. Since Fe_2O_3 and Fe-rich iron molybdates are very unselective catalysts, it is generally accepted that oxygen is inserted into the activated propene molecule from Mo centers, with iron playing the role of a re-oxidizing agent. Also, given that in the absence of tellurium $Fe_2(MoO_4)_3$ is much less active and has a very low selectivity to acrolein, it seems reasonable to propose that Te promotes the α-hydrogen abstractor and is responsible for the high selectivity, but also participates to the redox process, thus necessarily implying the participation of the Te^{4+}/Te^{2+} redox couple. The XPS study of the FeMoTeO-SiO_2 catalyst provided no clear evidence of the formation of

reduced species of these elements. This is possibly due to the presence of Fe^{3+} centers, which are easily reduced and promote the rapid re-oxidation of the intermediate species.

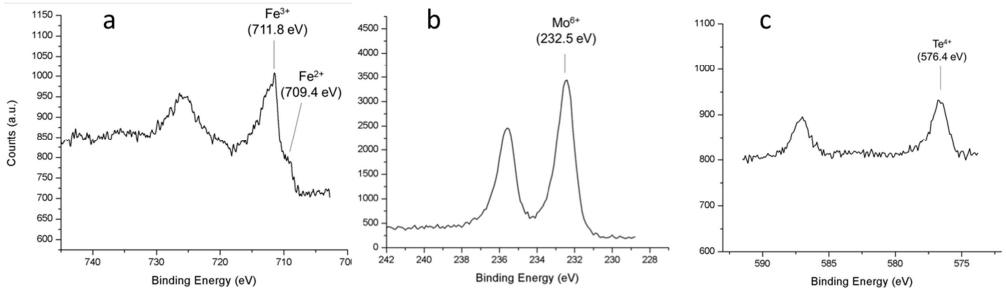

Fig. 11: XPS spectra for the FeMoTeO-SiO_2 sample in the Fe 2p (a), Mo 3d (b) and Te 3d (c) regions after in situ reduction by propene.

For this reason, we undertook a similar XPS study of the reduction of MoTeO catalysts, in an effort to observe the redox properties of their surface in the absence of iron. The reduction was carried out following the same protocol as that described for the FeTeMoO-SiO_2 catalysts. Since in the case of the MoTeO catalysts, the highest selectivity to acrolein was observed in the first hours of reaction, we implemented the propene pulse test on the surface of the fresh catalyst. As shown in Fig. 12, it is immediately evident that, following its exposure to propene, the surface was strongly reduced, with a strong peak at 231.5 eV attributed to the Mo^{5+} species and a smaller one at 229.5 eV attributed to the Mo^{4+} species [51,52], an asymmetric feature was observed on the high BE sides, which was most probably due to a charging effect of the surface, since it was also observed on the Te3d and O1s peaks. In this respect, it is important to note that MoO_3 is a good insulator, and that charging effects are not uncommon on such materials [35].

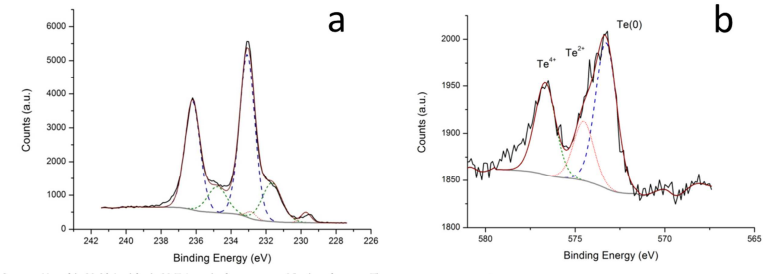

Fig. 12: XPS spectra for the MoTeO sample in the Mo 3d (a) and Te 3d (b) regions after in situ reduction by propene.

It can be seen that, following the propene pulse, a tenfold increase in the concentration of Mo^{5+} occurred. On the other hand, there was a very low level of molybdenum reduction to Mo^{4+}, which is often proposed as an intermediate species in the mechanism of propene oxidation, was very limited. This result implies that if Mo^{4+} species are actually formed in the reaction mechanism they are quickly re-oxidized by vicinal cations with a higher oxidation state, such as Mo^{6+} or Te^{4+} in the present case. Concerning tellurium, this element was found on the fresh catalyst, exclusively in the Te(IV) oxidation state on the fresh catalyst, as indicated by the presence of a single feature at 576.5 eV (Table 4). Following the propene pulse, a broad Te signal was obtained, composed of at least three different features at 573.0, 574.2 and 576.4 eV, as reported in Fig. 12. These peaks were identified, by comparison with reference data from the literature as Te^{4+}, Te^{2+} and Te(0) species respectively [22,43]. It can be noticed the presence of a shoulder at higher BE that was not fitted, since it was the result of a charging effect observed on all the XPS signals for this sample.

The detection of the Te^{2+} intermediate species is interesting since it has been previously observed in Mo-V-Te oxide catalysts used for the oxidation of propane where it takes part in the re-oxidation of vanadium [22]. The formation of metallic tellurium can thus be explained by the further reduction of Te^{2+} by propene or by the easy dismutation of Te^{2+} species into Te^{4+} and Te(0). Since Te(0) is highly volatile under standard operative conditions, this result could account for the deposition of metallic tellurium at the cold exit of the reactor when MoTeO catalysts are used, as reported by several authors [8,18]. This observation was further confirmed by the quantification, indicating that after the propene pulse, surface concentration of tellurium was halved and approximately half of the remaining tellurium was reduced to the Te(0) oxidation state.

To summarize, the aforementioned results describe the varying redox behaviors of iron, molybdenum and tellurium, which depend on the catalyst's composition, Table 6 lists the reduced species formed following exposure of the catalysts to a propene/air mixture, or propene pulses at the catalytic reaction temperature.

Table 6: Starting oxidation state of the constituting surface elements of the catalysts and reduced species formed in catalytic reaction conditions or after pulsing propene.

System	Starting oxidation state	Reduced species
FeMoO	Fe^{3+} Mo^{6+}	Mo^{5+}
FeMoTeO	Fe^{3+} Te^{4+} Mo^{6+}	Fe^{2+}
MoTeO	Te^{4+} Mo^{6+}	Te^{2+} Te^{0} Mo^{5+} Mo^{4+}

Since the values of formal potentials only can be found in the literature together with their variation as a function of the pH in the case of the solution chemistry of the redox couples, it is difficult to draw clear a conclusion concerning the behavior of these couples in solid-state catalysts. In addition, the redox potential of the Te^{4+}/Te^{2+} is unknown since the Te^{2+} state is unstable. However, on the basis of the measurements reported here and in accordance with the redox potentials published in the literature [53-55], it appears reasonable to propose the following hypotheses: The redox potential of Fe^{3+}/Fe^{2+} in the FeMoO did not allowed to re-oxidize the Mo^{5+} species in the amorphous layer supported on $Fe_2(MoO_4)_3$, which are formed upon oxidation of the propene molecules. This is due to the fact that both cations should have the same octahedral coordination and that consequently the redox potential of (Mo^{6+}/Mo^{5+}) falls below that of iron (Fe^{3+}/Fe^{2+}) [56].

When tellurium is introduced as a dopant in the MoTeO catalyst, the re-oxidation of the surface Mo^{5+} species is carried out by the Te^{4+}/Te^{2+} redox couple. Since Te^{2+} is an unstable species known to disproportionate to Te^{4+} and Te(0) [53], elemental tellurium is formed at the surface of the MoTeO catalyst and it is then easily volatilized. However, when iron is added to the catalyst (FeMoTeO), the close vicinity of Fe^{3+} cations to the partially reduced Te^{2+} allows for

fast re-oxidation of the latter species. This re-oxidation is rapid, and the Te^{2+} species could be expected in very low concentrations. They have never been detected in *in-situ* or *operando* conditions up to now, with the exception of the MoVTeNbO system [22]. The following redox process can thus be proposed:

$$Te^{4+} + 2\ Mo^{5+} \rightleftharpoons Te^{2+} + 2\ Mo^{6+} \qquad (2)$$

$$2\ Fe^{3+} + Te^{2+} \rightleftharpoons 2\ Fe^{2+} + Te^{4+} \qquad (3)$$

In accordance with the latter mechanism, the presence of iron would be beneficial since it drastically reduces the kinetics of the tellurium loss, by preventing the formation of surface Te(0) species. Similar Fe^{3+}/Fe^{2+} redox couple effects have already been demonstrated in the past. In this regard, the addition of cerium (Ce^{4+}/Ce^{3+}) or copper (Cu^{2+}/Cu^{+}), has also proven to be efficient in the suppression or reduction of Te volatilization [8,15,43]. Indeed, the influence of iron is not limited to this role as it also allows tellurium to re-oxidize molybdenum, thereby avoiding strong reduction of the later, and promoting a higher catalytic activity. Ultimately, besides its conventional role as an efficient alkene α-abstracting element, tellurium may thus also play an intermediary role between iron and molybdenum and the three Fe^{3+}/Fe^{2+}, Te^{4+}/Te^{2+} and Mo^{6+}/ Mo^{5+} redox couples work in synergy in a rather unique way. Indeed, the same three element redox cooperation should not take place in the $Bi_3FeMo_2O_{12}$ phase that could correspond to a comparable case since the respective coordination of Fe and Mo in the phase should allow a direct electron exchange between Fe and Mo. Besides, it is tempting to draw a parallel with the iron molybdate catalysts used in the oxidative dehydrogenation of methanol. If iron alone was shown in the current study not to intervene in the re-oxidation of molybdenum, it may not be the case in the oxidative dehydrogenation of methanol. Methanol has a higher reducing power and molybdenum at the surface is easily reduced to Mo^{4+} and another redox couple may have to be considered allowing Fe to take part directly in the re-oxidation of molybdenum. Furthermore, water intervenes with the formation of $MoO_2(OH)_2$ species not observed in the present case.

Conclusions

In this research, three catalysts containing either: iron and molybdenum, tellurium and molybdenum or all three elements together, have been studied as catalysts. These catalysts comprise a bulk $Fe_2(MoO_4)_3$ or MoO_3 phase, depending on whether iron is present or not, with a 5 and 10 nm thick amorphous surface layer containing either two or three of the elements. The redox state dynamics at the surface of the catalysts have been studied using surface and bulk spectroscopic techniques, in an effort to gain insight into the drastic improvement brought about by the addition of tellurium.

The results of this study indicate that, in addition to its basic role as an α-hydrogen abstraction promotor, which is essential for the selectivity to acrolein, tellurium plays a role of relay, allowing iron to intervene, thanks to its redox couple, in the re-oxidation of the molybdenum on the surface and thus to avoid a too deep reduction of the latter detrimental to the activity of the catalyst. The role of the Te^{4+}/Te^{2+} redox couple is thus highlighted for the first time and the positive role of iron in the stabilization of tellurium at the surface explained. This research also shows for the first time how three elements can work in perfect symbiosis, to form a very effective catalyst, which could open the door to the development of new, more sophisticated, efficient and stable oxidation catalysts.

Acknowledgment

ADISSEO company is gratefully acknowledged for financial support as well as O. Safonova from the Paul Scherrer Institute for her help in the recording of XANES spectra and P. Delichere from IRCELYON for useful and productive discussions about LEIS.

References

[1] M. Boudard, Effects of Surface Structure on Catalytic Activity. Proc. 6th Int. Congress on Catalysis, G. C. Bond G.C.: Wells P. B.; Tompkins F. C. Eds. The Chemical Society, London, 1 (1977) 1-9.

[2] J.C. Vedrine, G. Coudurier, J.M.M. Millet, Molecular Design of Active Sites in partial Oxidation Reactions on Metallic Oxides. Catal. Today 33 (1997) 3-13.

[3] R. Schlögl, Concepts in Selective Oxidation of Small Alkane Molecules Modern Heterogeneous Oxidation Catalysis: Design, Reactions and Characterization Edt N. Mizuno, Copyright WILEY-VCH Verlag GmbH & Co. KGaA, Weinheim (2009) 1-40.

[4] J.B. Wagner, O. Timpe, F.A. Hamid, A. Trunschke, U. Wild, D. S. Su, R. K. Widi, S. Bee Abd Hamid, R. Schlögl, Surface Texturing of Mo–V–Te–Nb–O_X Selective Oxidation Catalysts, Top. Catal., 2006, 38, 51-58.

[5] J.F. Brazdil, L.C. Glaezer, R.K. Grasselli, An Investigation of the Role of Bismuth and Defect Cation Vacancies in Selective Oxidation and Ammoxidation Catalysis. J. Catal. 81 (1983) 142-146.

[6] A. Getsoian, V. Shapovalov, A.T. Bell, DFT+U Investigation of Propene Oxidation over Bismuth Molybdate: Active Sites, Reaction Intermediates, and the Role of Bismuth. J. Phys. Chem. C 117 (2013) 7123-7137.

[7] R.K. Grasselli, G. Centi, F. Trifiro, Selective Oxidation of Hydrocarbons Employing Tellurium Containing Heterogeneous Catalysts. Appl. Catal. 57 (1990) 149-166.

[8] W. Ueda, Y. Moro-oka, T. Ikawa, Study of Tellurium Oxide Catalysts by $^{18}O_2$ Tracer in the Oxidation of Propylene to Acrolein. J. Catal. 88(1984) 214-221.

[9] Y.H. Taufiq-Yap, S.N. Asrina, G.J. Hutchings, N.F. Dummer, J.K. Bartley, Effect of Tellurium Promoter on Vanadium Phosphate Catalyst for partial Oxidation of n-butane. J. Natural Gas Chem. 20 (2011) 635-638.

[10] Q. Huynh, Y. Schuurman, P. Delichere, S. Loridant, J.M.M. Millet, Study of Te and V as Counter-cations in Keggin type Phosphomolybdic Polyoxometalate Catalysts for Isobutane Oxidation. J. Catal. 261(2009) 166-176.

[11] P. Forzatti, P.L. Villa, D. Ercoli, G. Ercoli, F. Gasparini, F. Trifiro, Molybdates doped with tellurium as oxidation catalysts. Prod. RD 16(1977) 26-35.

[12] Y.N. Shyr, G.L. Price, Tellurium Mixed Oxide Selective Oxidation Catalysts. I. Kinetic Investigation. Ind. Eng. Chem. Prod. Res. Dev. 23(1984) 536-541.

[13] Y.N. Shyr, G.L. Price, Tellurium Mixed Oxide Selective Oxidation Catalysts. I. Catalyst characterization. Ind. Eng. Chem. Prod. Res. Dev. 23(1984) 542-545.

[14] A.A. Firsova, A.Y. Aleksandrov, I.P. Suzdalev, L.Y. Margolis, λ-resonance Spectroscopic Study of State of Tellurium in Cobalt Molybdate. Bull. Acad. Sci. USSR Div. Chem. Sci. 22 (1973) 2106-2108.

[15] J.C.J. Bart, N. Giordano, Structure and Activity of Tellurium-Molybdenum Oxide Acrylonitrile Catalysts. J. Catal. 64 (1980) 356-370.

[16] J.C.J. Bart, A. Bossi, P. Perissinoto, A. Castellan, N. Giordano, Some Observations on the Thermochemistry of Telluric Acid. J. Therm. Anal. 8 (1975) 313-327.

[17] M.A.K. Ahmed, H. Fjellväg, A. Kjekshus, Synthesis, Structure and Thermal Stability of Tellurium oxides and Oxide Sulfate formed from Reactions in refluxing sulfuric acid. J. Chem. Soc. Dalton Trans. (2000) 4542-4549.

[18] A. Castellan, A. Vaghi, J.C.J. Bart, N. Giordano, Propylene Oxidation on TeO_2-SiO_2 Catalysts. J. Catal. 39 (1975) 213-224.

[19] J. Nilsson, A. Landa-Canovas, S. Hansen, A. Andersson, Catalysis and Structure of the $SbVO_4/Sb_2O_4$ System for Propane Ammoxidation. Catal. Today 33 (1997) 97-108.

[20] R.K. Grasselli, C.G. Lugmair, A.F. Volpe Jr, Towards an Understanding of the Reaction Pathways in Propane Ammoxidation Based on the Distribution of Elements at the Active Centers of the M1 Phase of the MoV(Nb,Ta)TeO. Top. Catal. 54 (2011) 595-604.

[21] J.M.M. Millet, H. Roussel, A. Pigamo, J.L. Dubois, J.C. Jumas, Characterization of Tellurium in MoVTeNbO Catalysts for Propane Oxidation or Ammoxidation. Appl. Catal. A: Gen. 232 (2002) 77-92.

[22] B. Deniau, T.T. Nguyen, P. Delichere, O. Safonova, J.M.M. Millet, Redox State Dynamics at the Surface of MoVTe(Sb)NbO M1 Phase in Selective Oxidation of Light Alkanes. Top. Catal. 56 (2013) 1952-1962.

[23] O.V. Safonova, B. Deniau, J.M.M. Millet, Mechanism of the Oxidation-Reduction of the MoVSbNbO Catalyst: In Operando X-ray Absorption Spectroscopy and Electrical Conductivity Measurements. J. Phys. Chem. B 110 (2006) 23962-23967.

[24] Y. Zhu, P.V. Ushko, D. Melzer, E. Jensen, L. Kovarik, C. Ophus, M. Sanchez-Sanchez, J.A. Lercher, N.D. Browning, Formation of Oxygen Radical Sites on MoVNbTeOx by Cooperative Electron Redistribution. JACS 139 (2017) 12342-12345.

[25] M. Tonelli, M. Aouine, V. Belliere Baca, J.M.M. Millet, Selective Oxidation of Propene to Acrolein on FeMoTeO Catalysts: Determination of Active Phase and Enhancement of Catalytic Activity and Stability. Catal. Sci. Technol. 7 (2017) 4629-4639.

[26] A.I. Vogel, G. Svehla, Vogel's Textbook of Macro and Semimacro Qualitative Inorganic Analysis, 5th edition, Longman, (1996)

[27] Database: Inorganic Crystal Structure Database, ICSD. In Release 2008

[28] J.M.M. Millet, C. Virely, M. Forissier, P. Bussiere, J.C. Vedrine, Mössbauer Spectroscopic Study of Iron Phosphates Catalysts used in Selective Oxidation. Hyperfine Interact. 46 (1989) 619-628.

[29] M. Tonelli, Design of new Catalysts for the mild Oxidation of Propene to Acrolein. PhD Thesis 325-2015 Claude-Bernard University Lyon 1 (2015).

[30] E. Söderhjelm, M.P. House, N. Cruise, J. Holmberg, M. Bowker, J.O. Bovin, A. Andersson, On the Synergy Effect in MoO_3–$Fe_2(MoO_4)_3$ Catalysts for Methanol Oxidation to Formaldehyde. Top. Catal. 50 (2008) 145-155.

[31] K. Routray, W. Zhou, J.C. Kiely, W. Grünert, I.E. Wachs, Origin of the Synergistic Interaction between MoO_3 and Iron Molybdate for the Selective Oxidation of Methanol to Formaldehyde. J. Catal. 275 (2010) 84-98.

[32] C. Brookes, P.P. Wells, N. Dimitratos, W. Jones, E.K. Gibson, D.J. Morgan, G. Cibin, C. Nicklin, D. Mora-Fonz, D.O. Scanlon, C.R.A. Catlow, M.J. Bowker, The Nature of the Molybdenum Surface in Iron Molybdate. The Active Phase in Selective Methanol Oxidation. Phys. Chem. C 118 (1014) 26155-26161.

[33] P. Forzatti, P.L. Villa, N. Ferlazzo, D. Jones, Multicomponent Catalysts for the Oxidation of Propylene to Acrolein: $Fe_2(MoO_4)_3$ doped with Bi or Te. J. Catal. 76 (1982) 188-207.

[34] J. Baltrusaitis, B. Mendoza-Sanchez, V. Fernandez, R. Veenstra, N. Dukstiene, A. Roberts, N. Fairley, Generalized Molybdenum Oxide Surface Chemical State XPS Determination via Informed Amorphous Sample Model. Appl. Surf. Sci. 326 (2015) 151-161.

[35] C.V. Ramana, V.V. Atuchin, V.G. Kesler, V.A. Kochubey, L.D. Pokrovsky, V. Shutthanandan, U. Becker, R.C. Ewing, Growth and Surface Characterization of Sputter-deposited Molybdenum Oxide thin Films. Appl. Surf. Sci. 253 (2007) 5368-5374.

[36] A.P.S. Dias, F. Montemor, M.F. Portela, A. Kiennemann, The Role of the Supra-Stoichiometric Molybdenum during Methanol to Formaldehyde Oxidation over Mo-Fe mixed Oxides. J. Mol. Catal. Chem. 397 (2015) 93-98.

[37] K. Thavornprasert, M. Capron, L. Jalowiecki-Duhamel, O. Gardoll, M. Trentesaux, A.S. Mamede, G. Fang, J. Faye, N. Touati, H. Vezin, J.L. Dubois, J.L. Couturier, F. Dumeignil, Highly Productive Iron Molybdate Mixed Oxides and their Relevant Catalytic Properties for Direct Synthesis of 1,1-dimethoxymethane from Methanol. Appl. Catal. B: Env. 145 (2014) 126-135.

[38] T. Yamashita, P. Hayes, Analysis of XPS Spectra of Fe^{2+} and Fe^{3+} ions in Oxide Materials. Appl. Surf. Sci. 254 (2008) 2441-2449.

[39] H. Hayashi, N. Shigemoto, S. Sugiyama, N. Masaoka, K. Saitoh, X-ray Photoelectron Spectra for the Oxidation State of TeO_2-MoO_3 Catalyst in the Vapor-phase Selective Oxidation of Ethyl lactate to Pyruvate. Catal. Lett. 19 (1993) 273-277.

[40] X.L. Xiong, L.E. Cadus, L. Daza, P. Bertrand, J. Ladrière, P. Ruiz, B. Delmon, Reactivity of Iron Molybdate artificially Contaminated by Antimony ions and its Relation with Catalytic Activity in the Selective Oxidation of Isobutene to Methacrolein Top. Catal. 11-12 (2000) 167-180.

[41] Q. Xu, G. Jia, J. Zhang, Z. Feng, C. Li, Surface phase composition of iron molybdate Catalysts studied by UV Raman Spectroscopy. J. Phys. Chem. C 112 (2008) 9387-9393.

[42] P. Forzatti, P.L. Villa, N. Ferlazzo, D. Jones, Multicomponent Catalysts for the Oxidation of Propylene to Acrolein: $Fe_2(MoO_4)_3$ doped with Bi or Te. J. Catal. 76 (1982) 188-207.

[43] W. Ueda, Y. Moro-oka, T. Ikawa, Study of Multicomponent Bismuth Molybdate Catalysts by $^{18}O_2$ Tracer. Chem. Lett. 11 (1982) 483-486.

[44] S.N. Mikhailov, R.J.M. Elfrink, J.-P, Jacobs, L.C.A. van den Oetelaar, P.J. Scanlon and H.H. Brongersma, Quantification in low-energy ion scattering: elemental sensitivity factors and charge exchange processes, Nucl. Instr. And Meth. In Phys. Res. B93 (1994) 149-155.

[45] H.H. Brongersma, M. Draxler, M. de Ridder, P. Bauer, Surface composition analysis by low-energy ion scattering, Surface Science Reports 62 (2007) 63-109.

[46] L. Wu, W. Yang, A. Frenkel, I. Study of the Local Structure and Oxidation State of Iron in Complex Oxide catalysts for Propylene Ammoxidation. Catal. Sci. Technol. 4 (2014) 2512-2519.

[47] T. Ressler, O. Timpe, T. Neisius, J. Find, G. Mestl, M. Dieterle, R. Schlögl, Time-Resolved XAS Investigation of the Reduction/Oxidation of MoO_{3-x}. J. Catal. 191 (2000) 75-85.

[48] M.G. O'Brien, A.M. Beale, S.D.M. Jacques, B.M. Weckhuysen, A Combined Multi-Technique In Situ Approach Used to Probe the Stability of Iron Molybdate Catalysts During Redox Cycling. Top. Catal. 52 (2009) 1400-1409.

[49] F. Garagiola, S. Mobilio, P. Villa, G. Vlaic, Insertion of Dopant Te in $Fe_2(MoO_4)_3$ determined by Fluorescence EXAFS. Chim. Ind. 70 (1988) 78-81.

[50] A.P.V. Soares, M.F. Portela, A. Kiennemann, L. Hilaire, J.M.M. Millet, Iron Molybdate Catalysts for Methanol to Formaldehyde Oxidation: Effects of Mo Excess on Catalytic Behavior. Appl. Catal. A: Gen. 206 (2001) 221-229.

[51] A. Katrib, J.W. Sobczak, M. Krawczyk, L. Zommer, A. Benadda, A. Jablonski, G. Maire Surface studies and Catalytic Properties of the Bifunctional Bulk MoO_2 System. Surf. Interface Anal. 34(2002) 225-229.

[52] W. Ji, R. Shen, R.Yang, G. Yu, X. Guo, L. Peng, W. Ding, Partially Nitrided Molybdenum Trioxide with Promoted Performance as an Anode Material for Lithium-ion Batteries. J. Mater. Chem. A 2 (2013) 699-704.

[53] A.I. Alekperov, Electrochemistry of Selenium and Tellurium. Russ. Chem. Rev. 43 (1974) 235-250.

[54] V.G. Shcherbakov, Z.K. Stegendo, R.A. Antonovain, G.V. Samsonov (Ed.), Chem. Prop. Anal. Refract. Compd. Khimicheskie Svoistva Metody Anal. Tugoplavkikh Soedin. Химические Свойства И Методы Анализа Тугоплавких Соединений, Springer US, (1972) 91-93.

[55] D.M. Bouroushian in Electrochemistry of Metal Chalcogenides, Springer Berlin Heidelberg, (2010) 57-75.

[56] J.B. Goodenough, J.M. Longo J.M. Landolt-Bornstein Tabellen Neue Serie III/4a, SpingerVerlag, Berlin (1970).

FIGURES CAPTION

Fig. 1: X-ray diffraction patterns of the studied catalysts, a) FeMoO, b)FeMoTeO, c)FeMoTeO-SiO_2.Indexation of the peaks is given between 10 and 30°2θ.

Fig. 2: TEM images of the iron containing samples a) FeMoTeO and b) FeMoO.

Fig. 3: a) HRTEM image of particles of the MoTeO sample. b) STEM-EDX mapping of the Te and Mo elemental distribution for an examined area.

Fig. 4: Evolution over time on stream of the propene conversion (empty squares) and acrolein selectivity (full diamond) for the FeMoTeO sample (black) at 450°C, the FeMoO sample (green) at 450°C and MoTeO (red) at 360°C; other testing conditions: GHSV = 295 h^{-1}, $C_3H_6/O_2/N_2$ = 1:1.5:8.6.

Fig. 5: XPS spectra for The FeMoTeO and FeMoO samples in the Fe 2p region before (in black) and after catalytic testing (in blue).

Fig. 6: Semi-quantitative surface analyses carried out by XPS and LEIS accompanied by the ion dose calculations (a). Spectra of the FeMoTeO sample collected at 1 and 2 KeV after different times (b), (c) and (d).

Fig. 7: XANES spectra of the fresh and used FeMoTeO sample at Fe (a) and Mo K-edge. (b)

Fig. 8: XANES spectra of the fresh and used FeMoTeO sample at Fe (a) and Mo K-edge (b).

Fig. 9: XANES spectra of the fresh and used FeMoTeO (a) and of TeMoO (b) catalysts at Te L_1-edge; the spectrum of Te_2MoO_7 is added for comparison in (b).

Fig. 10: Mössbauer spectra of the iron catalysts after catalytic testing a) FeMoTeO b) FeMoO c) FeMoTeO-SiO_2; solid-lines are derived from a least-squares fits.

Fig. 11: XPS spectra for the FeMoTeO-SiO_2 sample in the Fe 2p (a), Mo 3d (b) and Te 3d (c) regions after in situ reduction by propene.

Fig. 12: XPS spectra for the MoTeO sample in the Mo 3d (a) and Te 3d (b) regions after in situ reduction by propene